

Thermal equilibration of samples for neutron scattering

TOBIAS K. HERMAN,^{a*} SARAH PARKS^{a,b} AND JULIA SCHERSCHLIGT^a

^a*National Institute of Standards and Technology, Gaithersburg, MD 20899 USA, and*

^b*University of Maryland, College Park, MD 20742 USA. E-mail: toby@ualberta.net*

(Received 0 XXXXXXXX 0000; accepted 0 XXXXXXXX 0000)

Abstract

Temperature relaxation and equilibration of samples for neutron scattering was investigated in a selection of samples and sample cells within the range of 5 K to 300 K. A simple model was developed that relates thermal relaxation time constants to material properties of the sample and sample cell. This model should facilitate extension of this study to prediction of thermal behavior in other systems.

1. Introduction

Neutron scattering probes bulk properties of macroscopic samples. To allow measurements of these properties at a range of temperatures neutron scattering facilities have developed large suites of sample environment equipment optimized for use in neutron beams, including cryostats for measurements far below room temperature. These cryostats are designed to minimize the material exposed to the neutron beam. Furthermore, the composition of the cryostat and sample cell material that is exposed to neutrons is chosen carefully – typical choices are aluminum (small neutron scattering cross-section, but with Bragg peaks appearing as background signal) or vanadium

(incoherent neutron scatterer, giving a featureless background). These two metals are also fairly good thermal conductors. Powder samples are usually packed into a hollow cylindrical cell, sealed with helium gas in the interstitial volume between grains (to allow thermal conduction through the sample), and mounted on cryostats. Single-crystal samples may be mounted similarly (in a hollow cell filled with exchange gas) or they may be mounted directly on the cryostat without any sample cell at all. Unfortunately, this optimization for neutron scattering can come at the expense of other considerations such as quick thermal equilibration.

Neutron scattering setups make it very difficult to directly measure the temperature of the sample itself, since one must keep all sensors and wiring out of the scattering region (the neutron beam). Sometimes a temperature sensor is mounted on the sample cell, but more often it is mounted on the sample stage of the cryostat itself. Therefore one cannot assume that the measured temperature truly reflects the sample temperature. Instead, some knowledge of the thermal properties of the sample and of the sample cell must be used to choose an appropriate wait time in order to allow the temperature of the sample to equilibrate with that of the cryostat's sample stage.

This paper outlines a series of measurements on the thermal equilibration of samples mounted in typical setups used at the National Institute of Standards and Technology (NIST) Center for Neutron Research (NCNR). The thermal response of the samples to a temperature step is characterized by a relaxation time constant, which can be used to suggest a waiting time to allow for sample equilibration to the new temperature set point. A number of different sample materials have been investigated, and three different sample cells were chosen from our selection of standard sample cells. While thermal relaxation time constants depend on both sample identity and sample cell construction, generalities emerge that can be used to predict the equilibration rate of

other samples.

Poorly prepared powder samples have been shown to exhibit very poor thermal equilibration (Ryan and Swainson, 2008), and may even produce spurious neutron signals (Chi *et al.*, 2011). In contrast, the samples investigated here were all properly prepared – the thermal time constants shown here are best case scenarios for these materials and sample cells. Powders loaded in an atmosphere containing significantly less helium gas will exhibit slower equilibration than seen here.

2. Experimental setup

2.1. Cryostat

The cryostat used in this study is a commercial cryocooler designed and built for neutron scattering; its useful temperature range spans 5 K to 325 K. The cryocooler is widely used for experiments at the NCNR and can be considered a canonical system for neutron scattering; this type of system is colloquially referred to as a “bottom loading CCR.” The space surrounding the sample cell is evacuated and the cell is directly bolted to the cryocooler sample stage. The only thermal contact between the sample stage and the sample cell is provided by conduction across the mounting surface where the sample cell lid abuts the copper sample stage. For this investigation, we restrict ourselves to exploring the thermal behavior of samples sealed in cans with helium exchange gas providing thermal contact between the sample and the sample can.

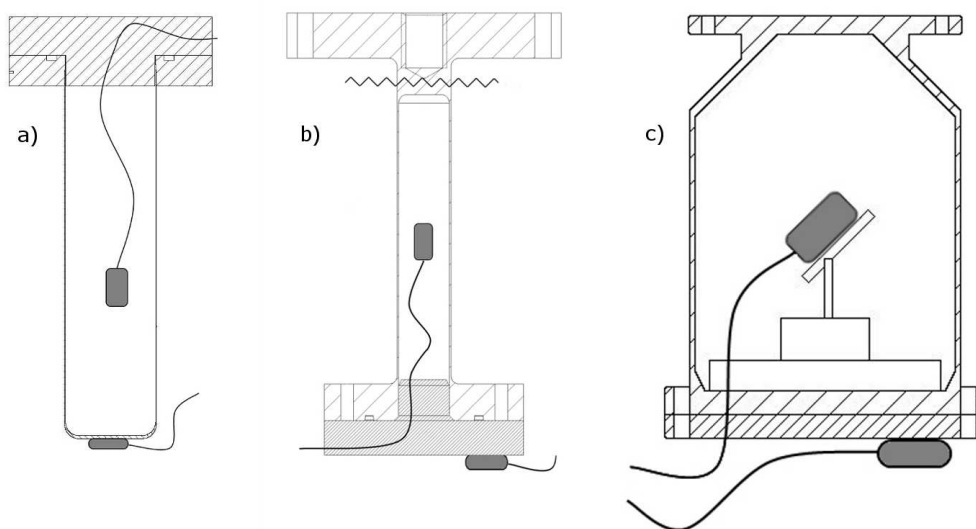
In typical operation, a sample is loaded and sealed with indium into a cell in a helium-rich environment. The cell is then leak tested to better than 5×10^{-6} mbar·l/s and bolted onto the copper sample stage of the cryocooler. The temperature of the sample stage is read by silicon diode temperature sensor bolted to the back of the sample stage. A commercial temperature controller is used to control the temperature

within the range of 5 K to 320 K by means of two canister heaters mounted in the sample stage. The sample cell is held against the sample stage by four screws, with a thin coating of vacuum grease on the sample stage for increased thermal contact.

2.2. Sample cells

There are two broad classes of powder sample cell at the NCNR: those with aluminum walls and those with vanadium walls. Both the vanadium and aluminum sample cells come in a range of sizes; the size chosen is usually dictated by the quantity of sample that is available and by the scattering cross section of the sample. Single-crystal sample cells come in many shapes and sizes; the one we study here is widely used at the NCNR. It is a large diameter can with a multiple position mount inside for aligning the single crystal with respect to the cell-

All these cells are displayed schematically in Fig. 1 and they all share certain characteristics: a large flange for bolting securely to the sample stage of the cryostat, an indium seal between the cell body and the cell lid to seal the helium exchange gas inside the cell, and thin walls in order to minimize neutron scattering from the cell itself. Dimensions of these cells are included in Table 1. We have modified these cells slightly to allow us to measure temperatures inside the sample, and at the base of the sample cell itself. Small holes were drilled through either the body of the cell or the lid and thermometer leads (32 AWG cryogenic wire) were epoxied in place to provide leak-tight electrical feedthroughs.



Schematics of the three types of cell studied in this paper (not drawn to scale): a) vanadium powder cell, b) aluminum powder cell and c) single-crystal cell. Each cell has an electrical feed-through leading to an internal temperature sensor, and a single external sensor mounted on the portion of the sample can furthest from the cryostat. Sensors are indicated by gray shaded regions.

	V powder cell	Al powder cell	Single crystal cell
Wall material	V	Al	Al
Wall thickness	0.15 mm (0.006")	0.25 mm (0.010")	0.65 mm (0.025")
Cell diameter	16 mm (0.625")	13 mm (0.500")	53 mm (2.1")
Cell length	65 mm (2.56")	57 mm (2.25")	61 mm (2.40")

Table 1 Dimensions of the sample cells used in this study

2.2.1. Vanadium powder cell The vanadium cell consists of a thin hollow cylinder of vanadium molded out of metal sheet and welded to an upper flange made of a titanium alloy (Ti-6Al-4V). The cell is sealed with an aluminum lid, which is mounted on the cryostat. This cell design is primarily used for powder diffraction experiments. The cell is pictured in Fig. 1a; relevant dimensions are included in Table 1. Both temperature sensors used in this cell were Si diodes, approximately 2 mm x 3 mm x 1 mm in size – the sensor on the base of the cell was varnished directly to the vanadium body.

2.2.2. Aluminum powder cell The body of the aluminum cell is machined from a single piece of material. It includes one flange that bolts to the cryostat and another sealed with an aluminum lid. This cell design is used for both diffraction and inelastic measurements. A standard cell is shown in Fig. 1b; relevant dimensions are included in Table 1. Another aluminum cell was altered to try to reduce its thermal response time – the upper flange was cut off at the zigzag line. This altered cell was sealed using a lid that has additional holes for mounting to the cryostat similar to the vanadium can. The internal sensors used in both cells were calibrated resistance temperature sensors, while the sensor on the base of the cell was a Si diode.

2.2.3. Single-crystal cell The single-crystal cell consists of a large hollow cylindrical lid which slips over a versatile base on which single-crystal samples can be mounted and aligned. Once the sample is manually aligned on the base, the upper portion of the cell is bolted over it in a helium rich environment and the entire assembly is bolted to the cryostat. For our study the single-crystal sample was replaced with a Si diode temperature sensor. A second Si diode temperature sensor was fixed to the bottom of the cell. This cell is shown in Fig. 1c; relevant dimensions for the cell are included in Table 1.

2.3. Sample material

We chose fiducial samples to represent two classes of materials commonly studied by neutron scattering. To represent metallic samples we chose lead (Pb) powder¹ since it is less flammable and easier to work with than most metal powders. To represent oxides and porous media we chose alumina (Al_2O_3)². Lead and alumina also represent extremes in Debye temperatures (Θ_D) that one could expect to encounter in samples

¹ 99%, 0.05 mm particle size

² 0.1 mm particle size, pore size 5.8 nm, specific surface area 155 m²/g

at 88 K (White and Meeson, 2002) and 1045 K (Wachtman *et al.*, 1962) respectively. Debye temperature is relevant since it characterizes the temperature dependence of heat capacity, which in turn affects the thermal equilibration of samples.

2.4. Temperature steps

The behavior of each sample was monitored after step changes in set temperature of the cryostat. Most data were collected after warming steps of $\Delta T = 10$ K, but to check for consistency, some data were taken using other step magnitudes. Warming and cooling data over the same range of temperatures were also compared. The size of the temperature step and the recent thermal history of the sample both affect thermal relaxation, but do not cause more than a few percent variation in the thermal relaxation rate except in the case of very large temperature steps (on the order of 100 K, data not shown).

3. Expected thermal behavior

3.1. Thermal equilibration model for sample

The temperature of a monolithic sample attached to a single heat source/sink (the cryostat) through a thermally resistive link relaxes exponentially to the temperature of the cryostat.

$$\frac{T_{sample}(t) - T_{cryostat}}{T_{sample}(0) - T_{cryostat}} = \exp(-t/\tau) \quad (1)$$

The time constant for this relaxation should equal the heat capacity, C , of the sample times the thermal resistance, R , of the link ($\tau = RC$).

In an ideal case, the cryostat would instantaneously reach some new temperature immediately after the set point is changed (i.e. $t = 0$). The sample temperature would then relax towards this new value according to Eq. 1. In reality cryostat equilibration takes a finite time and during that time the sample temperature will not relax

exponentially. The thermal time constants of the samples in this paper were extracted from data taken once the cryostat temperature equilibrated. Even once the cryostat temperature has reached the new set point, exponential relaxation of the sample temperature is not guaranteed since the model of the sample as a monolith connected to the cryostat through a thermal link is very simplistic.

In each of our setups, the upper flange of the cell is well anchored to the sample stage of the cryostat; it tracks the sample stage temperature throughout these experiments. A sudden change in temperature of the upper flange caused by a change in cryostat temperature propagates down through the walls of the sample cell. Thermal contact between the cell walls and the sample inside the cell is provided by helium exchange gas, allowing the sample to equilibrate to the new wall temperature. Thermal conductivity of various substances at low (10 K) and high (300 K) temperatures are included in Table 2 to help clarify the discussion that follows.

Material	Conductivity (W/mK)	
	10 K	300 K
Vanadium (a)	4.5	31
Aluminum 6061 (b)	14	155
Helium (c)	0.016	0.15
Lead (d)	18	35
Alumina, sintered (e)	5.6	50 (@200 K)

Table 2 Selected thermal conductivities of materials used in this study. References are: (a) Childs *et al.* 1973 (b) Marquart *et al.* 2000 (c) Lemmon *et al.* (d) Ho *et al.* 1968 (e) Touloukian and Buyco 1970

Conduction through the gas-filled powder will set the ultimate limit on the thermal equilibration rate, even once cell design is optimized. The effective conductivity of a gas-filled powder depends on the thermal properties of the powder and gas, the packing geometry (e.g. number of contact points between neighboring grains), the packing density and the size of the particles (Gusarov and Kovalev, 2009). Following this reference, we use our known particle size to estimate the effective conductivity of our prototypical powder samples to be about a factor of five greater than that of the helium exchange gas alone. This enhancement in conductivity over the conductivity of the exchange gas itself is gained because conduction through the individual powder

grains is quite fast – both lead and alumina have thermal conductivity orders of magnitude larger than that of helium gas, as seen in Table 2. The bottlenecks in heat transfer occur where these grains impinge on one another and energy must be transferred through the gas.

Since thermal conductance is proportional to conductivity and cross-sectional area, conduction through the sample parallel to the cell walls may contribute to heat flow between the sample and the cryostat if the cell walls are thin or constructed of a poor thermal conductor. Consider the vanadium cell in Table 1 at room temperature. The cells's very thin walls (0.15 mm) and the large cross-section of the gas filled powder sample within (16 mm diameter) lead to comparable thermal conductance through the walls and the powder respectively, despite the much larger thermal conductivity of the vanadium metal compared to helium gas. Thus, heat flows vertically through the sample as easily as it does through the cell walls. In contrast, the walls of the aluminum cell are thicker and made of a higher conductivity material, leading to a thermal conductance much larger than that of the powder sample – in this case heat flows through the walls much more effectively than it flows into or out of the sample.

Thermal conductance down the sample cell is not the only important factor in determining relaxation rate in Eq. 1 – heat capacity is just as important. While the vanadium cell body is pressed from a sheet of metal and therefore has a thin bottom, the aluminum cell is machined in such a way that a large mass of material remains at the bottom of the cell, adding to its heat capacity. For instance, the aluminum powder cell used in this study can hold 6.3 cm^3 of powder sample, but includes approximately 8 cm^3 of additional aluminum metal in the bottom flange and lid; in other words, there is more sample cell material to cool or warm than there is sample itself. We show below that this additional mass does indeed lead to thermal equilibration times much longer than the internal equilibration time of the sample.

Filled sample cells have a much more complex geometry and need not exhibit pure exponential relaxation. Nonetheless, in our analysis we found that fitting the time evolution of sample temperature to a pure exponential resulted in small fitting residuals in virtually all situations. Some data points could be fit much better using a stretched exponential (Kohlrausch-Williams-Watts function), but even then, the thermal time constants extracted by the two different fits agreed within a few percent. Since the goal of this study is to propose general guidelines, and variations between samples and sample cells far outweigh any variations due to fitting method, we have opted to analyze the data using the simpler exponential model.

During large changes in temperature, the choice of which data to include also affected the extracted time constants. If too large a range is included in the fit, the time constant may be changing within that temperature range; if too small a range is included the quality of the fit suffers, resulting in larger uncertainties. To remain consistent, sample data were fit only when they satisfied the following requirements:

1. The cryostat had stabilized within 0.5 K of the new set temperature
2. The sample temperature had stabilized within 5 K of the set temperature

These requirements are somewhat arbitrary – any number of alternative values for these cutoffs could have been chosen, as long as they remained constant to ensure consistency between data points.

3.2. Temperature dependence of thermal time constants

As stated earlier, the thermal relaxation time should scale roughly linearly with the heat capacity (C) and thermal resistance (R) of the sample and sample cell. We can model this behavior using the following expression:

$$\tau = RC = \frac{C}{K} \propto \frac{C_{sample} + C_{cell}}{K'_{sample} + K'_{cell}} \quad (2)$$

where K is the effective thermal conductance of the system which in turn depends on the area weighted conductivity K' of each component, defined as $K' = \kappa \times A$. This term can be thought of as the inverse of resistance per unit length; it takes into account both the thermal conductivity (κ) of the material and the cross sectional area (A) of the cell walls or sample. C is a simple sum of the heat capacities of the sample and of the sample cell. For aluminum sample cells thermal conduction occurs overwhelmingly through the walls of the cell and the K'_{sample} term can be ignored; however, in vanadium cells thermal conduction through the sample itself remains important as noted above.

For the purpose of this experiment, the Debye model of specific heat suffices to calculate C . Variations of a few percent between experimental runs are as great as any likely deviation of the true specific heat from the Debye model. Thus, each heat capacity term depends on the system temperature, T , and the Debye temperature, Θ_D , of the material. Thermal conductivities were taken from literature for aluminum 6061 (Marquart, *et al.*, 2000), vanadium (Childs *et al.*, 1973) and helium gas (Lemmon *et al.*, 2011). The thermal conductivity of the sample was assumed to be directly proportional to the conductivity of the helium exchange gas as discussed above.

Given the geometries of our sample cells it is difficult to predict the relative contributions of the heat capacities of the sample and cell – their magnitudes were left as adjustable parameters in our model, denoted as A_S and A_C respectively. The thermal time constant data for each sample were fit to the form:

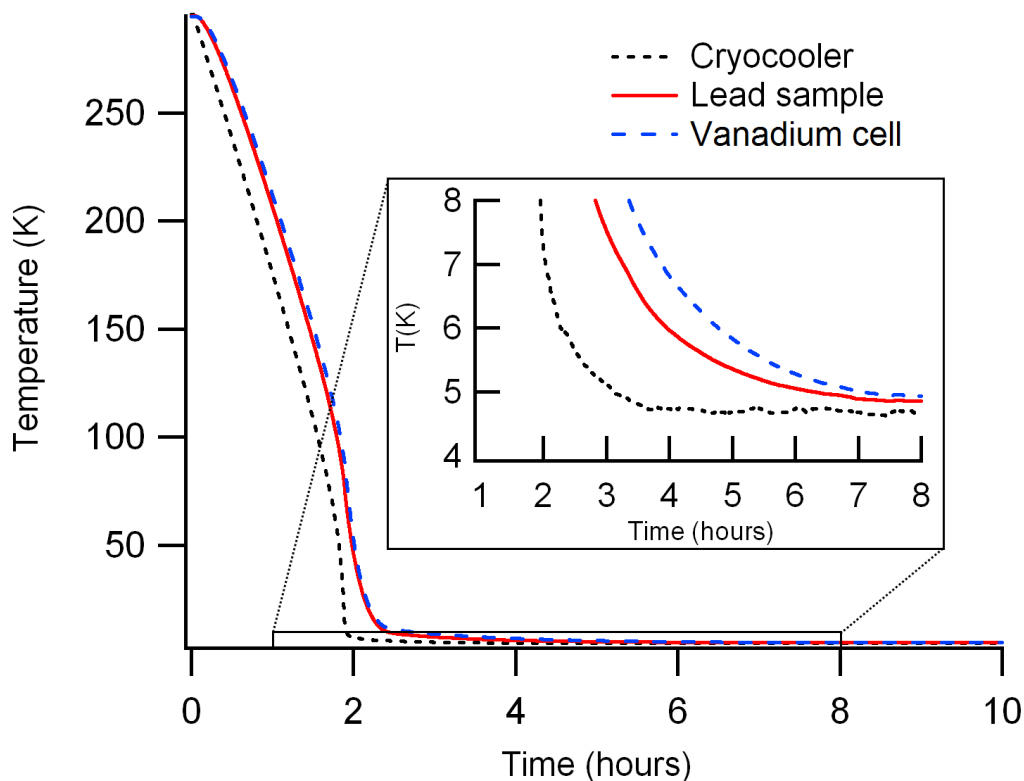
$$\tau = \frac{A_S C(T, \Theta_{D,S}) + A_C C(T, \Theta_{D,C})}{K'_S + K'_C} \quad (3)$$

where the subscripts S, C refer to the sample and sample cell respectively. This model has four adjustable parameters ($A_S, \Theta_{D,S}, A_C, \Theta_{D,C}$) – the Debye temperatures extracted from the fit can be compared to literature values to evaluate how appropriate this model is.

4. Results

4.1. Initial cool down

During many experiments the sample is initially cooled to the lowest temperature needed. Because the sample temperature can't be monitored directly, one might assume data collection can begin once the cryostat reaches its base temperature. However, sample temperature does not necessarily equilibrate at the same rate as the cryostat and can be far slower. The sample temperature initially tracks the cryostat temperature well (with an offset) as it cools. However the final few degrees of cooling, for the sample to reach the same temperature as the cryostat, takes a much longer time. For example, the cooling from room temperature of lead powder in a vanadium sample cell is shown in Fig. 2. While the cryostat has reached a temperature of 6 K after 2.5 hours, the sample temperature has not reached 6 K until 2 hours later – 4.5 hours after turning on the cryocooler. This slow relaxation has been seen in both the vanadium and aluminum cells – similar data for the temperature of NaCl in an aluminum cell (not shown) did not reach 6 K until an hour after the cryostat did. In each of the systems studied in this investigation, we see evidence of two conflated thermal relaxations, governed by separate relaxation rates. For clarity these are referred to as the major and minor relaxation processes. This paper focuses on the major relaxation process, which dominates in most instances. The minor relaxation process only becomes important once the temperature has relaxed to within about 1% of the temperature step to the new set point (e.g. within 100 mK of the new set point after a 10 K temperature step). The origin of this minor process is not clear. Except for very large temperature steps (such as the initial cool down), in most powder neutron scattering experiments it is more than sufficient to have equilibrated to within a percent of the temperature step, so the minor relaxation process can be ignored.

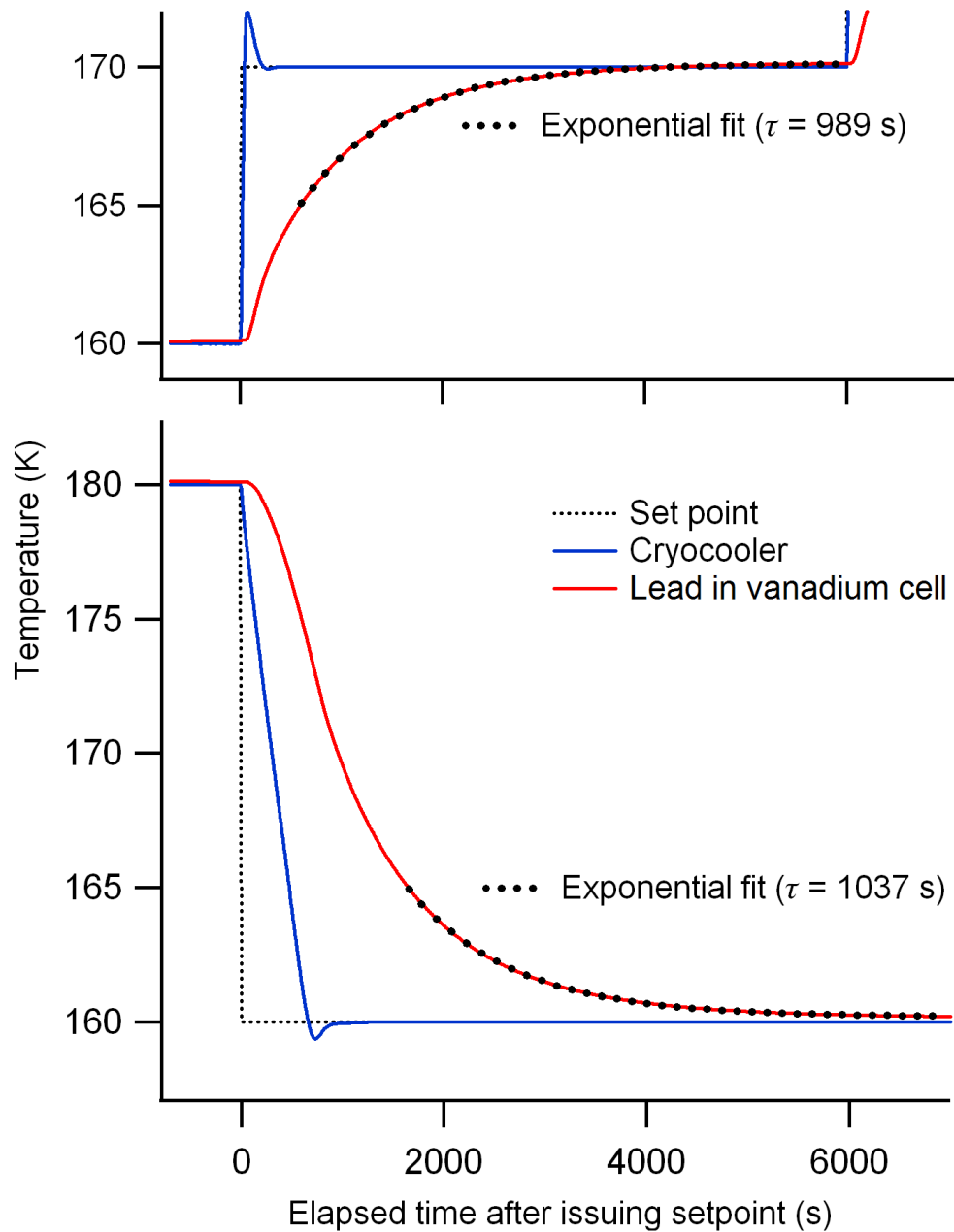


Initial cool down from room temperature of a lead powder sample in a vanadium cell. Note that the very slow “minor relaxation process” dominates as temperature falls below 8 K.

4.2. Typical thermal relaxation after a temperature step

In a typical neutron scattering experiment, cryostat temperature is changed abruptly and after a finite waiting time the sample is assumed to have equilibrated with the cryostat. In Fig. 3 we show two such steps for a sample in a vanadium cell. After a change of the set temperature from 160 K to 170 K, the cryostat temperature quickly equilibrates at the new set-point. The interior of the sample lags behind, reaching equilibrium much later. A simple exponential fit is included, yielding a thermal time constant of 989 seconds (16 minutes). The second step shown in the figure, cooling from 180 K to 160 K, shows a situation in which the finite time for the cryostat to reach its new temperature can affect the relaxation of the sample temperature – the

sample temperature does not decay exponentially at first, but it does become exponential once the cryostat temperature has equilibrated. The fit to this step yields a time constant of 1037 seconds (17 minutes—meaning that an experimenter who requires reasonably high accuracy must wait over half an hour for the sample to equilibrate after a temperature step of only a few degrees). Fits for data at all temperatures produced very small error bars for the time constants – usually just a few seconds. The difference between warming and cooling data here is statistically significant and illustrates the dependence on history and temperature step size.



Thermal behavior of a lead powder sample in a vanadium sample cell. The dotted lines correspond to simple exponential fits with a time constants of 989 and 1037 s respectively

4.3. Thermal equilibration in vanadium sample cells

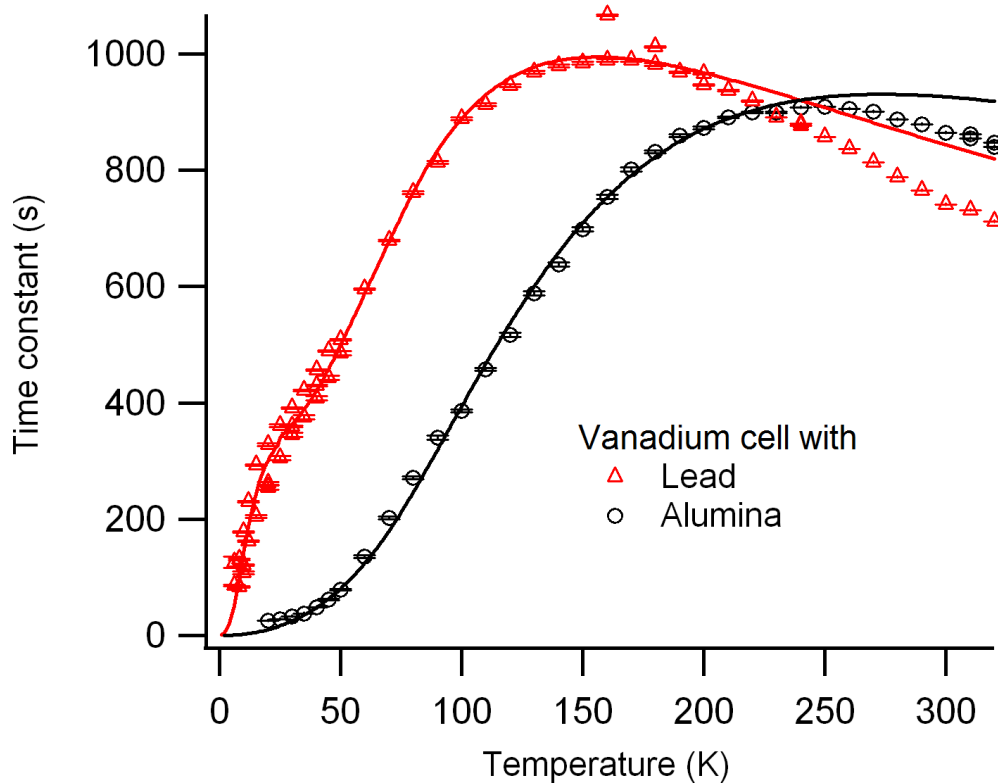
At low temperatures, where heat capacities are low, thermal response tends to be very quick, increasing with temperature before reaching a plateau at some moderate temperature. Data are shown for lead (Pb) and for alumina (Al_2O_3) powders in a vanadium sample cell in Fig. 4. The time constants near room temperature are quite comparable, but the low temperature response is very different. Lead, with its very low Debye temperature, has an appreciable heat capacity even at very low temperatures. Alumina, with its very high Debye temperature, has very little heat capacity at low temperatures and thus responds very quickly to any change in cryostat temperature. Data collected for sodium chloride are not shown, but fall between the data for lead and alumina.

Fits to Eq. 3 are included. While agreement is very good at low temperatures, there is a systematic deviation from the model at higher temperatures; only data below 200 K are used in the fit shown in Fig. 4. This model does an excellent job at low to moderate temperatures, even capturing the unexpected knee that is seen at around 20 K in the data for lead in Fig. 4. The failure of the model at high temperatures may be because only conductive heat transfer was considered, or may be because the values we use do not reflect the true conductivities of our vanadium cell – the literature values used are for purified elemental vanadium whereas our cells are made of commercial grade vanadium.

Adjusting the contribution of helium to the thermal conductivity of the powder sample (through a range of values consistent with the model of Gusarov and Kovalev (2009)) does not qualitatively change the fit. The choice of which data (warming, cooling or both; all temperatures, or just temperatures below 200 K) were included in the fit led to slight changes in fit parameters – for that reason it is difficult to place rigorous uncertainties to the Debye temperatures extracted from the fits. For the lead

sample, Debye temperatures from the fits were in the range 62 K - 83 K for the sample and 352 K - 395 K for the cell. These are close to the Debye temperatures of lead (88 K) and vanadium (380 K) (White and Meeson, 2002). The alumina sample could be satisfactorily fit with a single Debye temperature in the range 670 K - 703 K. This is midway between that of vanadium (380 K) and alumina (1045 K) – it is likely that the since all data were collected well below the Debye temperature of alumina the fits have trouble separating the contribution of alumina from that of the vanadium.

At all temperatures, relaxation of the temperature of the bottom at the sample cell itself has virtually the same time constant as that of the sample (data not shown), indicating that these time constants are set by the same factors. In other words, measuring the external temperature at the bottom of the cell is sufficient to determine the equilibration rate of the sample within the cell. Thus, conduction into the sample from the cell walls does not appear to be the limiting factor in thermal equilibrium in systems studied here, except in the special case of porous samples addressed later.

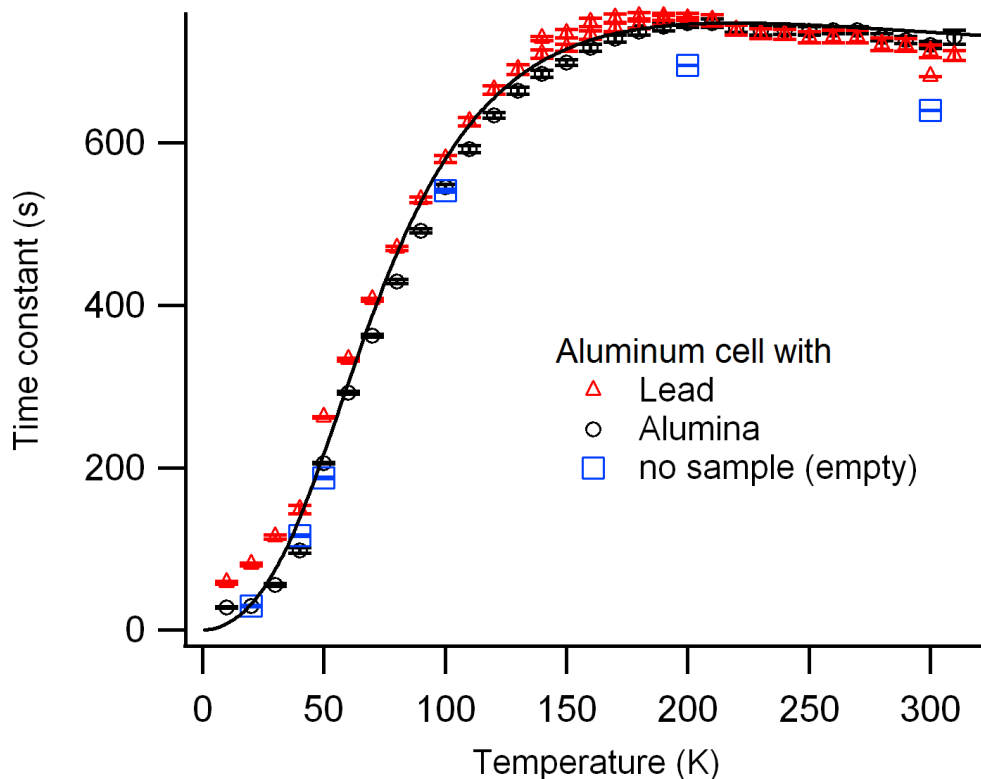


Time constants for samples in a vanadium sample cell. Fits are described in the text.

Error bars in this and all following figures are statistical error of fits (2 standard deviations) – they are smaller than the markers in most cases.

4.4. Thermal equilibration in aluminum sample cells

Time constants for lead and alumina samples in an aluminum sample cell are shown in Fig. 5. The time constants for both samples in this particular cell are virtually identical (except for some slight deviations at low temperature) indicating that the thermal response is completely dominated by the response of the cell itself. In fact, the empty cell responds only slightly faster than one filled with sample.

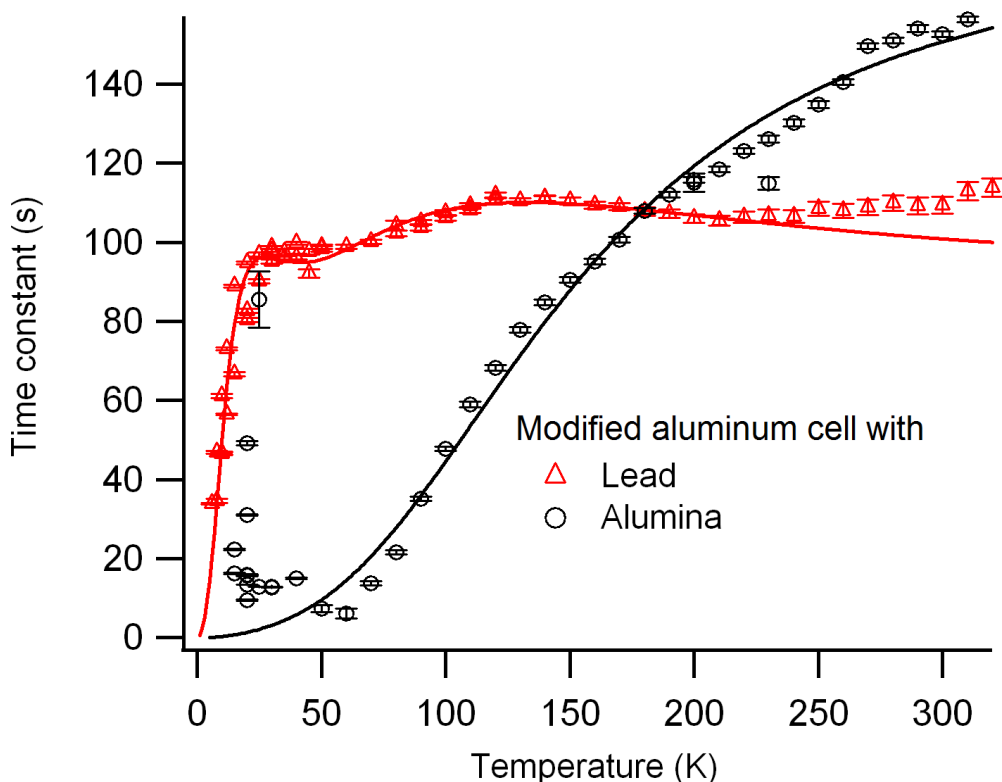


Time constants for an aluminum cell containing lead and alumina samples. Data for an empty aluminum cell are also included for a few temperatures.

The fit shown in Fig. 5 uses all data irrespective of sample identity and fits them with a single Debye temperature. Fits to these data yield Debye temperatures in the range 420 K - 460 K depending on whether all data or certain sub-sets are used. This is slightly high, but not unreasonable, for aluminum with its Debye temperature of 380 K (White and Meeson, 2002).

The small effect of changing sample material on the observed thermal time constants of the aluminum cell, and the long time constant of an empty cell, implies that the cell design itself is limiting the rate of thermal equilibration. To test this theory we removed the top flange completely and used the bottom flange to both seal the cell and mount it on the cryostat, reducing the aluminum at the base of the cell by about an order of magnitude. The resulting change in thermal behavior, shown in Fig. 6 was

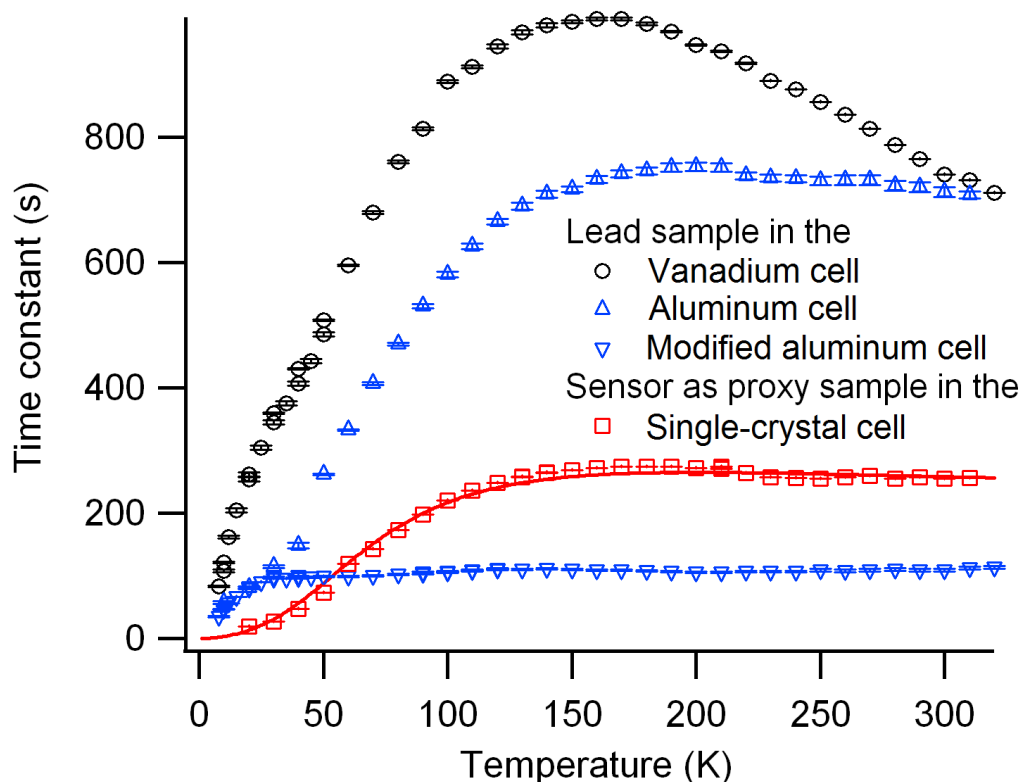
dramatic – time constants were reduced to a fraction of those of the unmodified cell. Furthermore, the identity of the sample became important in determining the temperature dependence of the thermal time constants, implying that the heat capacity of the cell no longer dominates the thermal behavior.



Time constants for a modified aluminum cell with lead and alumina samples.

Fits to Pb data below 200 K yield Debye temperatures in the 70 K - 80 K range for lead and 355 K - 405 K for aluminum – consistent with known values. If data at higher temperatures are included, the Debye temperature extracted for the sample cell rises to about 600 K – our model clearly is inadequate for temperatures above 200 K. Time constants for alumina are best fit with a single Debye temperature, as they were in the vanadium cell above; extracted Debye temperatures are in the range of 775 K - 930 K, intermediate between aluminum and alumina.

A comparison of time constants for the Pb sample in various sample cells is shown in Fig. 7; the single-crystal cell time constants are also included. The standard aluminum and vanadium cells have comparable response times at room temperature but the aluminum cell is clearly much faster at low temperatures. Both cells are much slower to equilibrate than a standard single-crystal sample cell. The modified aluminum cell is much more responsive than any other cell studied; in fact, powder samples in this cell actually equilibrate faster than the single-crystal sample at most temperatures.



Time constants for lead sample in all three powder cells. Also included is the response of the single-crystal cell, with fit to Eq. 3.

4.5. Special concerns for porous samples

Thermal conduction through powder samples relies on exchange gas filling the interstitial voids between particles. Conduction through direct particle-particle contacts is

extremely small – evacuated powders make exceptional thermal insulators. Helium makes an excellent exchange gas not just because of its intrinsically high thermal conductivity, but also because of its low boiling point and the fact that it does not freeze under atmospheric pressure (sealing a sample in a nitrogen environment, on the other hand, can lead to equilibration times on the order of days at low temperatures (Ryan and Swainson, 2009)). However, samples with very large surface areas (such as porous media) *can* adsorb helium at temperatures well above its boiling point. In fact this principle is used in cryogenics to create a ‘sorption pump.’ When a quantity of porous medium such as activated charcoal is cooled to 4 Kelvin it can adsorb a large quantity of helium gas – these so-called ‘sorbs’ can help maintain the high vacuum necessary inside ultra-low temperature cryogenic equipment for instance. At higher temperatures adsorption of gas is not energetically favorable; the temperature at which appreciable quantities of gas begin to adsorb depends on the identities of the substrate and gas

The alumina sample in this study began to adsorb the helium exchange gas at about 30 K, and by 5 K there appeared to be virtually no helium left in the voids between particles, as evidenced by the rising equilibration times at low temperature in Fig. 6. Additionally, without any exchange gas remaining outside of the alumina pores the sample temperature sensor was not well thermally coupled to the alumina sample in which it was embedded. The excitation current used to read the sensor in the vanadium cell (a Si diode) caused so much self heating that its temperature never fell below 10 K, even when the sample cell itself remained below 6 K for several hours as measured by an identical sensor mounted externally (data not shown). The RTD sensor in the aluminum cells dissipated much less energy during measurements and did not exhibit this self-heating. In this realm the thermal history of the sample becomes important – if the sample is warming, all the helium has already been adsorbed whereas if cooling,

some exchange gas may remain free long enough to help thermal equilibration. This is a well-known problem, but can be easily overlooked by neutron scatterers less familiar with cryogenics and/or porous media.

5. Conclusions

We have shown that it is possible to characterize the rate of thermal equilibration of samples studied by neutron scattering by a time constant. This time constant is *not* a prescription for how long to wait for thermal equilibration, but when the sample equilibrates more slowly than the cryostat it can be used to calculate an appropriate wait time before data collection by relating the acceptable error in temperature ($\delta T_{max} = T_{sample} - T_{set}$) to the size of a temperature change by:

$$\delta T_{max} = \left[T_{sample}^{(t=0)} - T_{cryostat} \right] \exp\left(\frac{-t_{wait}}{\tau}\right) \quad (4)$$

For samples with equilibration times of the same order as the cryostat equilibration times this relation becomes less useful, since relaxation deviates markedly from exponential – one must modify wait time based on experience.

The thermal time constants of the (internal) sample and (external) sample cell temperature sensors were virtually indistinguishable and the temperature dependence of these time constants is reasonably well described by a simple model. This suggests a straightforward procedure when one needs to characterize the thermal behavior of a new sample. Once a sample has been loaded into a sample cell, an external sensor can be used to measure the time constant at a few temperatures (possibly just one – room temperature) and these time constants can be used to predict the time constants over a much wider range by assuming reasonable values for the Debye temperatures of the sample and sample cell materials.

This type of study also provides a straightforward way to improve sample cell design. In the case of the aluminum cell studied here, a simple structural modification

improved its performance dramatically. For the vanadium cell no such simple modification is possible – however, if faster equilibration is desired, thicker walls can be used to increase the thermal conductance of the cell at the expense of more background in neutron scattering results.

Through maximizing the rate of equilibration through cell design, and providing accurate guidelines to experimenters based on empirical measurements, we can minimize the contribution of poor thermal equilibration to the uncertainty in our scattering data. We hope that similar measurements of other sample holders will lead to more reliable, and better characterized, thermal equilibration within all sample environment equipment.

The authors wish to thank Jeff Lynn, Judy Stalick, and Julie Borchers for fruitful discussions.

References

- E.D. Marquart, J.P. Le and R. Radebaugh *Cryogenic Material Properties Database*. NIST, 2000.
- A. V. Gusarov and E. P. Kovalev *Phys. Rev. B* **80**, 024202 (2009).
- G.K. White and P.J. Meeson *Experimental techniques in low-temperature physics*. Oxford University Press, 2002.
- J.B. Wachtman, Jr., W.E. Tefft, D.G. Lam, Jr., C.S. Apstein. *Phys. Rev.* **122**, 1754 (1962).
- G.E. Childs, L.J. Ericks and R.L. Powell *Thermal Conductivity of Solids at Room Temperature and below*, NBS Monograph 131, 1973.
- E.W. Lemmon, M.O. McLinden and D.G. Friend, "Thermophysical Properties of Fluid Systems" in **NIST Chemistry WebBook, NIST Standard Reference Database Number 69**, Eds. P.J. Linstrom and W.G. Mallard, National Institute of Standards and Technology, Gaithersburg MD, 20899, <http://webbook.nist.gov>, (retrieved October 7, 2011).
- C.Y. Ho, R.W. Powell and P.E. Liley *Thermal Conductivity of Selected Materials, Part 2*, NSRDS-NBS 16, 1968.
- Y.S. Touloukian and E.H. Buyco *Thermal conductivity, Volumes 1 and 2*, Plenum Press, 1970
- D.H. Ryan and I.P. Swainson *J. Appl. Cryst.* **42**, 43 (2009) .

S. Chi, J.W. Lynn, Y. Chem, W. Ratchiff II, B.g. Ueland, N.P. Butch, S.R. Saha, K. Kirshenbaum and J. Paglione *Meas. Sci. Technol.* **22**, 047001 (2011) .

Synopsis

Thermal equilibration rates are determined for typical powder samples used in neutron scattering experiments, at temperatures from 5 K to 300 K .
